Applied Physics Letters ARTICLE scitation.org/journal/apl

Demonstration of a compact x-ray free-electron laser using the optical klystron effect

Cite as: Appl. Phys. Lett. **119**, 151102 (2021); doi: 10.1063/5.0064934
Submitted: 28 July 2021 · Accepted: 23 September 2021 ·
Published Online: 11 October 2021

Eduard Prat,[a] Eugenio Ferrari, Marco Calvi, Romain Ganter, Sven Reiche, and Thomas Schmidt

AFFILIATIONS

Paul Scherrer Institut, CH-5232 Villigen PSI, Switzerland

[a]Author to whom correspondence should be addressed: eduard.prat@psi.ch

ABSTRACT

We demonstrate the operation of a compact x-ray free-electron laser (FEL) using the optical klystron mechanism. This effect speeds up the FEL process using the dispersion of magnetic chicanes placed between the undulator modules of the FEL beamline. The demonstration was performed at the soft x-ray beamline of SwissFEL, called Athos, which is, as far as we are aware, the only x-ray FEL to date with magnetic chicanes between every two undulator modules. In our measurements, we show that, compared to standard operation without chicanes, the required undulator length to achieve FEL saturation is reduced between 15% and 30% for radiation wavelengths between 1 and 2 nm. Fully exploiting the optical klystron effect represents an important step toward more compact FEL designs, rendering this key technology more affordable and hence accessible to a larger science community.

Linac-based x-ray free-electron lasers (FELs)[1–3] produce transversely coherent radiation with femtosecond duration and peak powers of tens of gigawatts and higher, enabling the examination of matter at atomic time and length scales. The unique properties of x-ray FELs have allowed observations of structural dynamics in proteins,[4–6] mechanisms regulating chemical bonds,[7,8] and the interaction between electronic and magnetic states related to information storage and energy conversion applications.[9–11]

Despite the unique research already demonstrated with such instruments, FEL science is a relatively young field with a strong potential to make revolutionary discoveries in the coming years. There are presently only a handful of available facilities to perform FEL science in the x-ray regime[12–18] with few more projects coming in the near future.[19,20] Most of the present and future facilities are based on the self-amplified spontaneous emission (SASE) mechanism,[21,22] although seeding schemes are implemented in several facilities to improve the longitudinal coherence with respect to the SASE-FEL pulses.[15,23–26] In this work we limit ourselves to SASE-FELs.

There is extensive worldwide research and development aiming at constructing more compact and cost-effective x-ray facilities. Examples of such efforts are the CompactLight project[27] and the ultracompact x-ray FEL initiative.[28] These projects intend to produce the required electron beam in compact accelerators with high-gradient technology and to employ short-period and compact undulator beamlines. Clearly, more compact designs for FEL facilities would lower their cost and render them accessible to a larger science community with corresponding benefits to society.

A fundamental contribution to the footprint and cost of x-ray FEL facilities is the undulator beamline. The undulator length required to produce high-power FEL radiation (the FEL saturation length) can be shortened significantly by applying the so-called optical klystron (OK).[29–37] Conversely, for a given undulator length, the OK may help us to achieve saturation for shorter wavelengths and to have more space to increase the FEL power via tapering of the undulator field.[38] Aside from allowing higher FEL powers and shorter radiation wavelengths, the OK configuration may be particularly relevant for special operation modes that require additional undulator space such as self-seeding[23,24] or the production of tunable two-color pulses in the so-called split-undulator configuration[39,40]—in both cases, the benefit of the OK is twofold, since two undulator sections are required instead of one.

The basic idea of the OK arose from developments in klystron rf technology. In FELs, it was initially proposed by Vinokurov and Skrinsky for FEL oscillators in the optical regime.[29] It has been extensively studied in FEL theory and simulations (see, e.g., Refs. 30–34). In the OK, magnetic chicanes between undulator modules are used to enhance the FEL process: the longitudinal dispersion R_{56} of the chicanes is used to effectively convert energy modulation to density modulation, thus speeding up the generation of microbunching that takes place during the FEL process. The OK process can be repeated several

times during the FEL amplification process. In general, more stages will allow a higher efficiency of the OK in reducing the saturation length: magnetic chicanes should be included after every undulator (before FEL saturation is reached) for a full exploitation of the OK.

The OK performance is very sensitive to the uncorrelated energy spread of the electron beam.[32,34] The energy spread effectively causes a Landau damping spreading any current modulation present in the electron distribution, thus counteracting the bunch formation by the OK. The uncorrelated relative energy spread σ_δ needs to be smaller than the Pierce or FEL parameter ρ[22] (with typical values between 10^{-3} and 10^{-4} for x-ray FELs), and the power gain of the OK will be higher for lower σ_δ/ρ ratios. From the one-dimensional FEL theory,[34] the maximum power gain of the single-stage OK (two undulators and one chicane) occurs when

$$\frac{2\pi}{\lambda} R_{56}^{*} \sigma_\delta \approx 1, \tag{1}$$

with λ being the FEL radiation wavelength. Therefore, the OK can be used to reconstruct the electron beam energy spread by finding the optimum longitudinal dispersion R_{56}^{*} for which the power gain of the OK is maximum.

The OK was first demonstrated in storage ring FEL oscillators such as the Duke FEL.[35] In linac-based SASE FELs, it has been demonstrated with a single stage in a VUV-FEL[36] and later with two and three stages for wavelengths entering the soft x-ray regime.[37] Here, we demonstrate the reduction of the saturation length in an x-ray FEL using the OK distributed along the full undulator beamline. The demonstration was performed in Athos, the soft x-ray beamline of SwissFEL at the Paul Scherrer Institute in Villigen, Switzerland.[41] Athos is the only x-ray FEL facility to date with magnetic chicanes between every two undulator modules, which is a requirement for fully exploiting the OK. We show that the saturation length in Athos is shortened between 15% and 30% for radiation wavelengths of 1 and 2 nm, respectively.

Figure 1 shows a sketch of Athos. Athos is based on short APPLE-X undulators[42,43] with alternating magnetic chicanes, allowing special operation modes for better control of FEL properties such as bandwidth and peak power. Athos, currently under final installation and standard commissioning, is planned to start user operation by the end of 2021. The beamline consists of 16 APPLE-X undulator modules capable of providing variable polarization and transverse gradient. The undulators have a period of 38 mm and a maximum undulator deflection parameter K of 3.8. In the final configuration, the electron beam energy at the undulator will be tunable between 2.9 and 3.4 GeV. This corresponds, for an undulator parameter K between 1 and 3.8, to a photon wavelength between 0.65 and 5 nm. The undulator length of each module is 2 m, which is the result of an optimization to give the best FEL performance for different operation modes including the OK configuration.[44] The space between the undulator modules is 0.8 m,

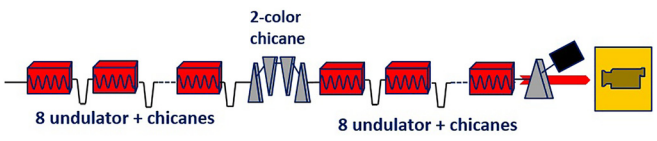

FIG. 1. Schematic layout of Athos, the soft x-ray beamline of SwissFEL.

hosting a quadrupole magnet to focus the electron beam, dipole corrector magnets to control the electron beam trajectory, electron beam diagnostics, vacuum components, and a compact magnetic chicane. There is an additional two-meter magnetic chicane installed in the middle of the undulator beamline to allow the generation of tunable two-color FEL pulses.[39,40] More information about Athos can be found in Ref. 41 and references herein.

The magnetic chicanes consist of four dipole permanent magnets occupying a total distance of 0.2 m. The chicanes introduce longitudinal dispersion (R_{56}) and a delay to the electron beam (with respect to the co-propagating radiation field) with R_{56} corresponding to approximately twice the delay. The R_{56} helps one to speed up the FEL process and to reduce the saturation length via the OK, the subject matter of this Letter. As envisaged in Athos, the delay can also be employed to improve the longitudinal coherence of the FEL radiation using the high-brightness SASE concept[45] to produce high-power and short pulses[46–50] and to generate phase-locked FEL pulses.[51] Each half of the chicane is motorized separately, allowing the generation of a transverse offset when one half has a different gap than the other. This feature, together with the dipole corrector magnet installed next to the chicane, gives independent control of the offset and angle of the electron beam trajectory, which is not critical for the OK but relevant to generate short and high-power FEL pulses with the tilted beam method.[48,50] The chicanes can provide a maximum delay of 2.4 μm and a transverse offset of ± 400 μm, which are rather large values for its compact length of 0.2 m and more than sufficient for their design purposes.[44] On top of the delay and offset, the chicanes have sufficient precision to control the delay on a sub-wavelength scale, and thus acting as a phase matcher. We note that a standard phase shifter would occupy a length of around 10 cm, so the additional space required for the chicanes (with a total length of 20 cm) is also around 10 cm.

We have measured the impact of the OK at Athos with 14 undulator modules for radiation wavelengths of 1.1 and 2.2 nm. The measurements took place in one experimental shift with equivalent conditions. Time-resolved measurements of the electron beam using an rf transverse deflector were not yet possible at Athos due to hardware still missing at the time of the experiment. Based on measurements at the hard x-ray beamline, we estimate the rms pulse duration of the electron beam to be around 40 fs with a peak current at the beam core of around 1.5 kA. The projected normalized emittance at the Athos beamline was measured around 500 nm. From measurements at the hard x-ray beamline,[52] the slice emittance is expected to be at the 200 nm level. We set optics to have an average β-function in the undulator between 6 and 7 m. The electron beam energy was 3.17 GeV. The undulators were set in circular polarization with K values tuned to 1.60 and 2.66 for FEL wavelengths of 1.1 and 2.2 nm, respectively. The radiation pulse energy was measured with a gas-based photon beam intensity monitor.[53]

The electron beam energy spread effectively increases due to the FEL process, and therefore the OK becomes less efficient and the optimum delays have to be reduced along the undulator beamline [see Eq. (1)]. Based on this, the optimization for the OK configuration is done as follows: (1) we start with the minimum number of undulator modules that give a reliable pulse energy reading in the gas detector (a few hundred nanojoules); (2) we tune the delays of the active chicanes (all set simultaneously) and set the optimum value; (3) we add one or two undulator modules; (4) we scan the new active chicanes and set

the resulting optimum; (5) we repeat steps 3 and 4 until a non-zero delay no longer increases the FEL power; (6) we close one by one the remaining undulators and optimize the phases between them.

For a radiation wavelength of 1.1 nm, we started with the first five undulators, and we simultaneously scanned the delays of the first four chicanes. The optimum delay was about 0.35 μm, giving a pulse energy of 1.2 μJ. We then closed the next two undulators and simultaneously scanned the corresponding chicanes, obtaining a maximum pulse energy of 17 μJ for a delay of 0.21 μm. We then activated the next undulator module and scanned the corresponding chicane, obtaining a maximum of 48 μJ for a delay of 0.1 μm. The rest of the chicanes were set around the minimum delay at the phase matching condition. For the 2.2 nm case, we started with the first three undulators and scanned the first two chicanes. The optimum delay was 0.7 μm, giving a pulse energy of 0.45 μJ. We repeated the same procedure but with four undulators and three chicanes, obtaining a maximum of 13 μJ for 0.65 μm delay—as mentioned earlier, since the FEL process increases the effective electron beam energy spread, it is expected that the optimum delay R^*_{56} decreases with more chicanes [see Eq. (1)]. We set the delays of the three chicanes based on the last scan. We then closed the fourth undulator and scanned the third chicane, obtaining a pulse energy of 110 μJ for an optimum delay of 0.2 μm. The rest of the chicanes were set to minimum delay and only acted as phase matchers.

Figure 2 shows examples of the delay scans for the first active chicanes and the final configuration of the chicane delays for the two radiation wavelengths. From the delay scans of the first part of the undulator, we can derive the energy spread of the electron beam using Eq. (1). (Here, we assume that the OK optimum for the first chicanes is equivalent to the one of a single chicane, although, as mentioned before, it could be slightly different due to the effective increase in energy spread associated with the FEL process.) For a radiation wavelength of 1.1 nm, $R^*_{56} = 0.7$ μm (the optimum longitudinal dispersion is twice the optimum delay of 0.35 μm), giving an absolute energy spread of 800 keV. Equivalent results are obtained for 2.2 nm and the optimum delay of 0.7 μm ($R^*_{56} = 1.4$ μm), as determined by scanning the first two chicanes.

Figure 3 shows measured and simulated gain curves with and without OK for radiation wavelengths of 1.1 and 2.2 nm. The measurements of the final pulse energies were about 0.7 and 1 mJ for radiation wavelengths of 1.1 and 2.2 nm, respectively. In the measurements, we optimized the linear taper amplitude after FEL saturation for each individual case. The simulation results were obtained with the code Genesis 1.3[54] As input, we used the measured or estimated beam parameters mentioned above. We assume that 80% of the electron bunch is contributing to the FEL process. The simulation results agree fairly well with the experimental data. Most importantly, the improved performances related to the OK are equivalent in measurements and simulations. The large discrepancies observed after saturation of the FEL process, especially for the 2.2 nm case, may be attributed to a non-optimum post-saturation taper configuration in the measurements.

It is evident from Fig. 3 that the FEL exponential growth starts substantially earlier, and the FEL saturation length is significantly

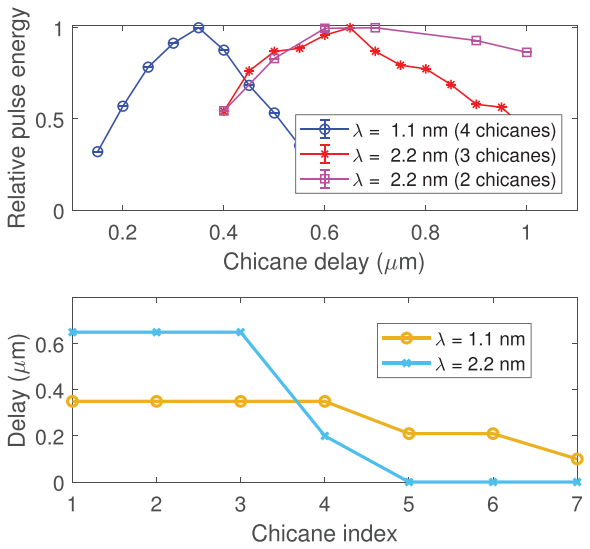

FIG. 2. Top: delay scans for the first chicanes for radiation wavelengths of 1.1 and 2.2 nm (the FEL pulse energy is normalized to the maximum). Bottom: final configuration of chicane delays for the two radiation wavelengths.

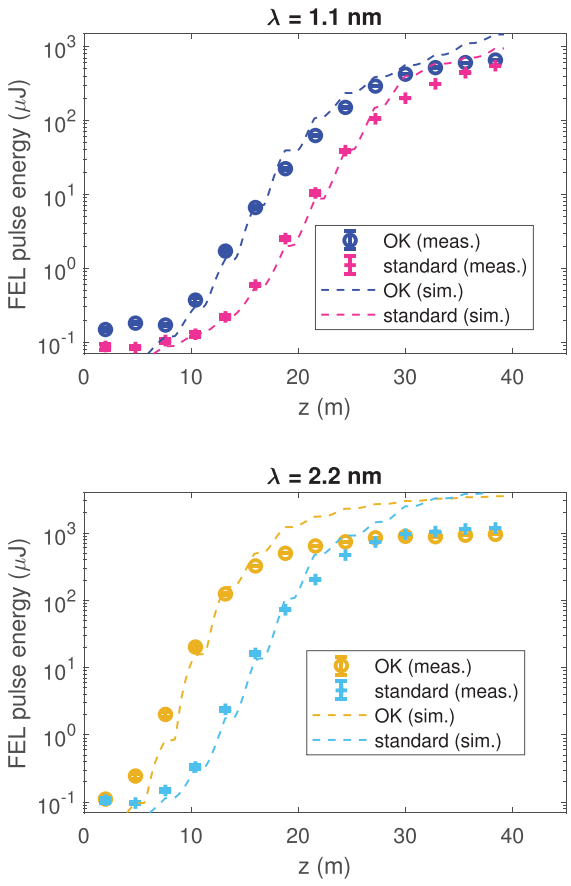

FIG. 3. Measured (meas.) and simulated (sim.) gain curves with and without OK configuration for radiation wavelengths of 1.1 nm (top) and 2.2 nm (bottom). z indicates the length along the undulator beamline.

reduced when applying the OK configuration. For the sake of a quantitative comparison, we arbitrary define as a measure for the saturation length the position along the undulator line, where the FEL pulse energy reaches a level of 300 μJ, close to the saturation pulse energy. For a radiation wavelength of 1.1 nm, this is achieved with ten undulator modules (corresponding to $z = 28$ m in the figure) with the OK, while 12 modules are required for the standard SASE configuration. For the 2.2 nm case, six modules are required when using the OK, while between eight and nine modules are needed without this enhancing effect. The exact saturation lengths, obtained by extrapolating the measurement data, are 32.5 m (without OK) and 27.4 m (with OK) for a radiation wavelength of 1.1 nm, and 22.6 m (without OK) and 15.7 m (with OK) for 2.2 nm. In relative terms, the undulator length is shortened by 16% for a radiation wavelength of 1.1 nm and 31% for 2.2 nm. Considering that the chicanes require an additional space of 0.1 m with respect to a standard phase shifter, the total reduction in footprint compared to an undulator beamline without chicanes would be 13% for 1.1 nm and 28% for 2.2 nm.

The performance of the OK, as mentioned earlier, strongly depends on the electron beam energy spread. The reconstructed value of 800 keV significantly exceeds the 350–500 keV range assumed in previous simulation studies for peak currents of 2–3 kA.[44,55] The large energy spread may be attributed to microbunching instabilities or intra-beam scattering. It was found to be sizable already in the gun/injector section, as reported in Ref. 56 and may be further increased during compression and transport down to the undulator entrance.

To better understand the sensitivity of the OK to the electron beam energy spread, we have simulated the effect of the OK for a radiation wavelength of 1.1 nm as a function of the energy spread. We have scanned the energy spread between 100 and 1200 keV—corresponding to relative values between 3.2×10^{-5} and 3.8×10^{-4}. The other parameters are equal to the ones in the measurements and simulations reported above. The FEL parameter for the simulated parameters is 2×10^{-3}. For each energy spread value, we set the optimum delay according to Eq. (1) for the chicanes up to FEL saturation. (For 800 keV, this matches the experimental value of 0.35 μm.) The simulation results are displayed in Fig. 4. While the FEL performance without OK improves only slightly with smaller values of the energy spread, a much stronger dependence is observed for the OK cases. For 100 keV, the saturation length is reduced by a factor of two, while for 1000 keV or larger, the OK is hardly beneficial at all. These simulations show that the impact of the OK may be much more important than presented here—either at other facilities with more favorable σ_δ/ρ ratios than in our case or in Athos if the energy spread can be improved in the future.

To conclude, we have demonstrated that the OK can be used to significantly reduce the saturation length of x-ray FEL facilities. Although our work deals with SASE-FEL pulses, the OK could potentially be used to reduce the saturation length for seeded FELs as well. The demonstration was performed at Athos, which is, as far as we are aware, the only x-ray FEL to date that can take full advantage of the OK by having magnetic chicanes between every two undulator modules. We have shown that the saturation length can be reduced between 15% and 30% for radiation wavelengths between 1 and 2 nm. Further improvements could be achieved with electron beams of lower energy spread. Our work shows that it is possible to construct x-ray FELs with significantly reduced undulator footprint and cost by fully exploiting the OK—an important advance in the quest for more compact and affordable FEL designs with the potential of expanding the FEL science community.

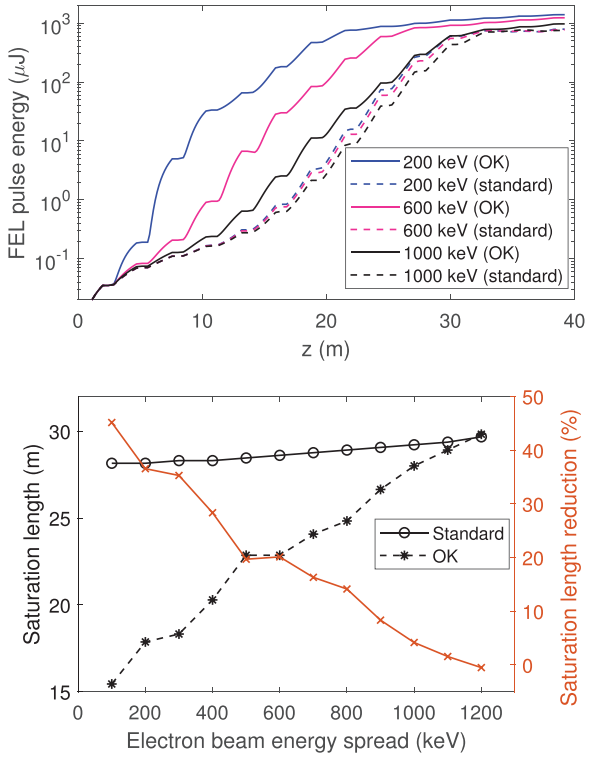

FIG. 4. Simulation of FEL performance for a radiation wavelength of 1.1 nm with and without OK and for different assumptions for the electron beam energy spread. Top: simulated FEL gain curves for energy spreads of 200, 600, and 1000 keV. Bottom: saturation length with and without OK (left axis) and saturation length improvement (right axis) as a function of the energy spread.

Future efforts at Athos may include improving the energy spread for a higher OK efficiency as well as the implementation of the OK for conditions requiring longer undulator lengths than shown here; e.g., for shorter radiation wavelengths and for special operation modes such as the generation of two-color FEL pulses using the split-undulator configuration.

We thank Thomas Schietinger for improving the language of the manuscript. We acknowledge the support of all the technical groups involved in the operation of SwissFEL.

DATA AVAILABILITY

The data that support the findings of this study are available from the corresponding author upon reasonable request.

REFERENCES

[1]Z. Huang and K.-J. Kim, Phys. Rev. Spec. Top. - Accel. Beams **10**, 034801 (2007).
[2]B. W. J. McNeil and N. R. Thompson, Nat. Photonics **4**, 814 (2010).
[3]C. Pellegrini, A. Marinelli, and S. Reiche, Rev. Mod. Phys. **88**, 015006 (2016).

[4]J. Kern, R. Alonso-Mori, R. Tran, J. Hattne, R. J. Gildea, N. Echols, C. Glockner, J. Hellmich, H. Laksmono, R. G. Sierra *et al.*, Science **340**, 491 (2013).
[5]E. Nango, A. Royant, M. Kubo, T. Nakane, C. Wickstrand, T. Kimura, T. Tanaka, K. Tono, C. Song, R. Tanaka *et al.*, Science **354**, 1552 (2016).
[6]P. Nogly, T. Weinert, D. James, S. Carbajo, D. Ozerov, A. Furrer, D. Gashi, V. Borin, P. Skopintsev, K. Jaeger *et al.*, Science **361**, eaat0094 (2018).
[7]M. Dell'Angela, T. Anniyev, M. Beye, R. Coffee, A. Fohlisch, J. Gladh, T. Katayama, S. Kaya, O. Krupin, J. LaRue *et al.*, Science **339**, 1302 (2013).
[8]H. Öström, H. Öberg, H. Xin, J. LaRue, M. Beye, M. Dell'Angela, J. Gladh, M. L. Ng, J. A. Sellberg, S. Kaya *et al.*, Science **347**, 978 (2015).
[9]C. E. Graves, A. H. Reid, T. Wang, B. Wu, S. de Jong, K. Vahaplar, I. Radu, D. P. Bernstein, M. Messerschmidt, L. Müller *et al.*, Nat. Mater. **12**, 293 (2013).
[10]P. Beaud, A. Caviezel, S. O. Mariager, L. Rettig, G. Ingold, C. Dornes, S.-W. Huang, J. A. Johnson, M. Radovic, T. Huber *et al.*, Nat. Mater. **13**, 923 (2014).
[11]C. Dornes, Y. Acremann, M. Savoini, M. Kubli, M. J. Neugebauer, E. Abreu, L. Huber, G. Lantz, C. A. F. Vaz, H. Lemke *et al.*, Nature **565**, 209 (2019).
[12]W. Ackermann, G. Asova, V. Ayvazyan, A. Azima, N. Baboi, J. Bähr, V. Balandin, B. Beutner, A. Brandt, A. Bolzmann *et al.*, Nat. Photonics **1**, 336 (2007).
[13]P. Emma, R. Akre, J. Arthur, R. Bionta, C. Bostedt, J. Bozek, A. Brachmann, P. Bucksbaum, R. Coffee, F.-J. Decker *et al.*, Nat. Photonics **4**, 641 (2010).
[14]T. Ishikawa, H. Aoyagi, T. Asaka, Y. Asano, N. Azumi, T. Bizen, H. Ego, K. Fukami, T. Fukui, Y. Furukawa *et al.*, Nat. Photonics **6**, 540 (2012).
[15]E. Allaria, D. Castronovo, P. Cinquegrana, P. Craievich, M. D. Forno, M. B. Danailov, G. D'Auria, A. Demidovich, G. D. Ninno, S. D. Mitri *et al.*, Nat. Photonics **7**, 913 (2013).
[16]H.-S. Kang, C.-K. Min, H. Heo, C. Kim, H. Yang, G. Kim, I. Nam, S. Y. Baek, H.-J. Choi, G. Mun *et al.*, Nat. Photonics **11**, 708 (2017).
[17]W. Decking, S. Abeghyan, P. Abramian, A. Abramsky, A. Aguirre, C. Albrecht, P. Alou, M. Altarelli, P. Altmann, K. Amyan *et al.*, Nat. Photonics **14**, 391 (2020).
[18]E. Prat, R. Abela, M. Aiba, A. Alarcon, J. Alex, Y. Arbelo, C. Arrell, V. Arsov, C. Bacellar, C. Beard *et al.*, Nat. Photonics **14**, 748 (2020).
[19]J. Galayda, in Proceedings of the 9th International Particle Accelerator Conference (IPAC2018), Canada (2018).
[20]Z. Zhao, D. Wang, Z.-H. Yang, and L. Yin, in Proceedings of the 38th International Free Electron Laser Conference (FEL2017), USA (2018).
[21]A. M. Kondratenko and E. L. Saldin, Part. Accel. **10**, 207 (1980).
[22]R. Bonifacio, C. Pellegrini, and L. M. Narducci, Opt. Commun **50**, 373 (1984).
[23]J. Amann, W. Berg, V. Blank, F.-J. Decker, Y. Ding, P. Emma, Y. Feng, J. Frisch, D. Fritz, J. Hastings *et al.*, Nat. Photonics **6**, 693 (2012).
[24]D. Ratner, R. Abela, J. Amann, C. Behrens, D. Bohler, G. Bouchard, C. Bostedt, M. Boyes, K. Chow, D. Cocco *et al.*, Phys. Rev. Lett. **114**, 054801 (2015).
[25]I. Inoue, T. Osaka, T. Hara, T. Tanaka, T. Inagaki, T. Fukui, S. Goto, Y. Inubushi, H. Kimura, R. Kinjo *et al.*, Nat. Photonics **13**, 319 (2019).
[26]I. Nam, C.-K. Min, B. Oh, G. Kim, D. Na, Y. J. Suh, H. Yang, M. H. Cho, C. Kim, M.-J. Kim *et al.*, Nat. Photonics **15**, 435 (2021).
[27]G. D'Auria, M. Aicheler, A. Aksoy, D. Alesini, R. Apsimon, J. M. Arnesano, M. Bellaveglia, A. Bernhard, F. Bosco, B. Buonomo *et al.*, in Proceedings of the 39th Free Electron Laser Conference (FEL2019), Germany (2019).
[28]J. B. Rosenzweig, N. Majernik, R. R. Robles, G. Andonian, O. Camacho, A. Fukasawa, A. Kogar, G. Lawler, J. Miao, P. Musumeci *et al.*, New J. Phys. **22**, 093067 (2020).
[29]N. A. Vinokurov and A. N. Skrinsky, BINP Report 77-59, BINP (1977).
[30]R. Coisson, Part. Accel. **11**, 245 (1981).
[31]P. Elleaume, J. Phys. Coll. **44**, C1 (1983).
[32]R. Bonifacio, R. Corsini, and P. Pierini, Phys. Rev. A **45**, 4091 (1992).
[33]E. L. Saldin, E. A. Schneidmiller, and M. V. Yurkov, DESY Report 03-108, DESY (2003).
[34]Y. Ding, P. Emma, Z. Huang, and V. Kumar, Phys. Rev. Spec. Top. - Accel. Beams **9**, 070702 (2006).
[35]Y. K. Wu, N. A. Vinokurov, S. Mikhailov, J. Li, and V. Popov, Phys. Rev. Lett. **96**, 224801 (2006).
[36]G. Penco, E. Allaria, G. D. Ninno, E. Ferrari, and L. Giannessi, Phys. Rev. Lett. **114**, 013901 (2015).
[37]G. Penco, E. Allaria, G. D. Ninno, E. Ferrari, L. Giannessi, E. Roussel, and S. Spampinati, Photonics **4**, 15 (2017).
[38]N. Kroll, P. Morton, and M. Rosenbluth, IEEE J. Quantum Electron. **17**, 1436 (1981).
[39]S. Reiche and E. Prat, J. Synchrotron Radiat. **23**, 869 (2016).
[40]A. A. Lutman, T. J. Maxwell, J. P. MacArthur, M. W. Guetg, N. Berrah, R. N. Coffee, Y. Ding, Z. Huang, A. Marinelli, S. Moeller *et al.*, Nat. Photonics **10**, 745 (2016).
[41]R. Abela, A. Alarcon, J. Alex, C. Arrell, V. Arsov, S. Bettoni, M. Bopp, C. Bostedt, H.-H. Braun, M. Calvi *et al.*, J. Synchrotron Radiat. **26**, 1073 (2019).
[42]T. Schmidt and M. Calvi, Synchrotron Radiat. News **31**, 35 (2018).
[43]X. Liang, M. Calvi, M.-E. Couprie, R. Ganter, C. Kittel, N. Sammut, T. Schmidt, M. Valléau, and K. Zhang, Nucl. Instrum. Methods Phys. Res., Section A **987**, 164741 (2021).
[44]E. Prat, M. Calvi, R. Ganter, S. Reiche, T. Schietinger, and T. Schmidt, J. Synchrotron Radiat. **23**, 861 (2016).
[45]B. W. J. McNeil, N. R. Thompson, and D. J. Dunning, Phys. Rev. Lett. **110**, 134802 (2013).
[46]T. Tanaka, Phys. Rev. Lett. **110**, 084801 (2013).
[47]E. Prat and S. Reiche, Phys. Rev. Lett. **114**, 244801 (2015).
[48]E. Prat, F. Löhl, and S. Reiche, Phys. Rev. Spec. Top. Accel. Beams **18**, 100701 (2015).
[49]T. Tanaka, Y. W. Parc, Y. Kida, R. Kinjo, C. H. Shim, I. S. Ko, B. Kim, D. E. Kim, and E. Prat, J. Synchrotron Radiat. **23**, 1273 (2016).
[50]A. A. Lutman, M. W. Guetg, T. J. Maxwell, J. P. MacArthur, Y. Ding, C. Emma, J. Krzywinski, A. Marinelli, and Z. Huang, Phys. Rev. Lett. **120**, 264801 (2018).
[51]N. R. Thompson and B. W. J. McNeil, Phys. Rev. Lett. **100**, 203901 (2008).
[52]E. Prat, P. Dijkstal, M. Aiba, S. Bettoni, P. Craievich, E. Ferrari, R. Ischebeck, F. Löhl, A. Malyzhenkov, G. L. Orlandi *et al.*, Phys. Rev. Lett. **123**, 234801 (2019).
[53]K. Tiedtke, J. Feldhaus, U. Hahn, U. Jastrow, T. Nunez, T. Tschentscher, S. V. Bobashev, A. A. Sorokin, J. B. Hastings, S. Möller *et al.*, J. Appl. Phys. **103**, 094511 (2008).
[54]S. Reiche, Nucl. Instrum. Methods Phys. Res. A **429**, 243 (1999).
[55]E. Prat and S. Reiche, J. Synchrotron Radiat. **26**, 1085 (2019).
[56]E. Prat, P. Dijkstal, E. Ferrari, A. Malyzhenkov, and S. Reiche, Phys. Rev. Accel. Beams **23**, 090701 (2020).